DEM simulation of effect of confining pressure on ballast behaviour

Simulation MED de l'effet de la pression de confinement sur l'environnement du ballast

P.K. Thakur, B. Indraratna & J.S. Vinod
University of Wollongong, Wollongong, Australia

ABSTRACT

In this paper, an attempt has been made to investigate the influence of confining pressure on deformation and degradation behaviour of railway ballast using the Discrete Element Method (DEM). A novel approach has been employed to model the two dimensional projection of field size ballast particles as cluster of bonded particles. Bonded particles are held together by a bond, and debonding is considered as particle breakage. A series of cyclic loading simulations using DEM were carried out on an assembly of angular ballast particles at different confining pressures (10 kPa to 240 kPa). The results highlight that the development of axial strain during cyclic loading as a function of initial confining pressure and number of cycles. Very high axial strain and breakage of particles have been observed at low confining pressure (< 30 kPa) owing to dilative volumetric strain behaviour. In terms of particle breakage, there exists an optimum range of confining pressures where breakage is minimal. In addition, the evolution of particle displacement vectors explains the breakage mechanism and associated deformations during cyclic loading.

RÉSUMÉ

Dans ce papier, en utilisant la Méthode d'Élément Discrète (MED), nous essayons d'examiner l'influence de la pression de confinement sur la déformation et le comportement d'avilissement du ballast de la voie ferrée. Une nouvelle approche a été employée afin de modéliser les deux projections dimensionnelles de la taille du champ de particules du ballast, représenté par un groupe de particules liées. Les particules sont liées entre elles par un lien et le déliement est considéré comme une rupture de particule. Une série de simulations de chargement cycliques utilisant la MED a été effectuée sur un assemblage de particules de ballast angulaires à différentes pressions de confinement (de 10 kPa à 240 kPa). Les résultats ont mis en évidence, pendant le chargement cyclique, l'amplification de la tension axiale par rapport à la pression de confinement initiale et le nombres de cycles. Une tension axiale très élevée et la rupture de particule ont été observés à basse pression de confinement (< 30 kPa) dû à un comportement d'expansion de la tension volumétrique. En ce qui concerne la rupture de particules, il existe une gamme optimale de pressions de confinement où la rupture est minimale. De plus, l'évolution des vecteurs de déplacement de particule explique le mécanisme de rupture et les déformation associées pendant le chargement cyclique.

Keywords : railtracks, ballast, particle breakage, confining pressure, discrete element, cyclic loading

1 INTRODUCTION

Ballast breakage during static and cyclic load application is a well-known phenomenon and often observed in railway tracks (Selig & Waters 1994; Indraratna et al. 1998; Indraratna & Salim 2005; Lackenby et al. 2007). Indraratna et al. (1998) reported that maintenance and rehabilitation costs of railway tracks due to problems associated with ballast performance are substantial, and several millions of dollars are being spent annually to cope with this problem worldwide. In railway tracks, the confining (lateral) pressure is usually very low (5 - 40 kPa) relative to the vertical stress applied to the ballast layer (Indraratna et al. 2005). Due to low lateral confinement, various problems such as: spreading of ballast, breakage of ballast, track buckling etc. has been experienced. Therefore, it is imperative to explore ballast behaviour under various confining pressures for optimizing the performance of ballast and reducing the maintenance costs. Indraratna et al. (2005) studied the ballast behaviour under various confining pressures experimentally and reported the existence of optimum confining pressure. In this paper, an attempt has been made to study the influence of confining pressure (in the range of 10-240 kPa) on deformation and degradation of ballast using the Discrete Element Method (DEM) employing PFC^{2D} (Particle Flow Code in 2-Dimension, (Itasca 2003)) and compare the results with the experimental observations made by Indraratna et al. (2005). The basic advantage of DEM simulation is that it explains the underlying mechanisms of particle densification and degradation during static and cyclic loading which is very difficult to study through experiment.

Limited studies have been carried out using the Discrete Element Method (DEM) to investigate the cyclic behaviour of ballast capturing breakage (Lim & McDowell 2005; Lobo-Guerrero & Vallejo 2006; Lu & McDowell 2006; Hossain et al. 2007). Most original DEM applications do not allow particle breakage (Cundall & Strack 1979). Therefore, various modeling techniques have been adopted by researchers to simulate particle breakage as summarized below.

First method is to treat each particle as a cluster of bonded smaller particles. The bonds which held the particles in a cluster together can disintegrate during cyclic loading, represents breakage. This approach has been adopted by Harireche and McDowell (2003), Cheng et al. (2004), Lim and McDowell (2005), Lu and McDowell (2006), Bolton et al. (2008) and others.

The second method of simulating particle breakage is to replace the particles fulfilling a predefined failure criterion with an equivalent set of smaller particles, as adopted by Lobo-Guerrero and Vallejo (2006), Hossain et al. (2007), and Ben-Nun & Einav (2008).

The first method of particle breakage criterion has been adopted here and cyclic biaxial tests have been simulated on an assembly of angular ballast particles uniquely formulated for this investigation.

Proceedings of the 17th International Conference on Soil Mechanics and Geotechnical Engineering
M. Hamza et al. (Eds.)

doi:10.3233/978-1-60750-031-5-602

2 NUMERICAL SIMULATION

2.1 *Particle generation*

For modeling realistic two dimensional (2-D) projections of the ballast particles, fifteen representative ballast particles (in the range of 19 – 53 mm size) of different shapes (almost rectangular, circular and triangular) were selected. The sieve sizes considered were in accordance with Standard Australia (1996).

The photographs of each of the selected ballast particles were taken and the images were imported into AutoCAD in a single layer. The images were then filled with tangential circles in another layer and every circle was given an identification number (ID). Identification number (ID), radius and central coordinates of each circular particle were extracted from AutoCAD in order to generate 'Balls' in PFC^{2D}. Table 1 shows the photos of some typical ballast particles created for the DEM simulations. These irregular particles were assigned names such as R1, R2, R3 as shown in Table 1.

Table 1. Representative ballast particles

Sieve size	Ballast Particles	PFC Particles
Passing 53 mm and retaining 45 mm sieve	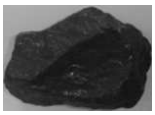	R1 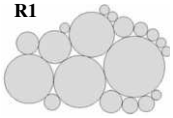
	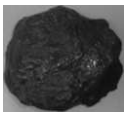	R2 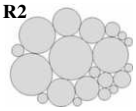
	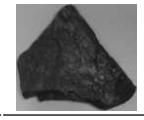	R3 

2.2 *Sample preparation*

Subroutines were developed (using the FISH Language) in PFC^{2D} after gathering the ID, radius, and coordinates of the centre of each circular particle representing angular ballast. These subroutines were used in the main program to generate irregular particles. A 300mm wide × 600 mm high biaxial cell (i.e. same size of laboratory) was generated for the DEM simulations and a typical sample is shown in Figure 1.

Table 2 lists the micromechanical parameters adopted for the DEM simulations. A linear contact model was used in these simulations.

In order to prevent particle breakage during the compaction stage, the ballast particles were treated as clumps (a group of particles which behave like a rigid body and have deformable boundaries) during isotropic stress installation (Itasca 2003). After the isotropic stress state, the clumps were released and parallel bonds (PB) were installed to make particles breakable. A parallel bond (PB) mimics the physical behaviour of a cement-like substance joining two particles.

2.3 *Cyclic load application*

A subroutine was developed to apply a stress-controlled cyclic biaxial test at the desired frequency (f) and amplitude of cyclic loading. The minimum cyclic stress (q_{min}) was kept at 45 kPa which represents the unloaded state of the track, such as the weight of sleepers and rails (Lackenby et al. 2007). The cyclic deviatoric stress (q_c) of 428 kPa was applied to the ballast which was estimated in accordance with Esveld (2001) assuming 30 ton axle load and 20 Hz frequency. Cyclic biaxial tests at a confining pressure (σ'_3) of 10 kPa, 30 kPa, 60kPa, 120 kPa and 240 kPa were simulated for 1,000 cycles. A frequency of 20 Hz, which corresponds to around 150 km/hr train speed on standard gauge track in Australia was applied to all the cyclic biaxial tests. Data such as axial strain (ε_a), volumetric strain (ε_v), bond breakage (B_r) were recorded after pre-determined number of cycles (N).

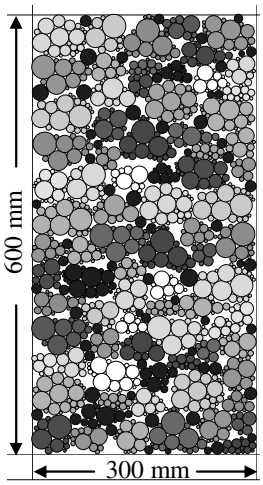

Figure 1. Initial assembly at σ'_3 = 10 kPa

Table 2 . Micromechanics parameters used in the DEM simulations

Micromechanics parameters	Values
Particle density (kg/m^3)	2500
Radius of particles (m)	16×10^{-3} – 1.8×10^{-3}
Interparticle & wall friction	0.4
Particle normal & shear contact stiffness (N/m)	3×10^8
Side wall Stiffness (N/m)	3×10^7
Top & bottom wall stiffness (N/m)	3×10^8
Parallel bond radius multiplier	0.5
Parallel bond normal & shear stiffness (N/m)	6×10^{10}
Parallel bond normal & shear strength (N/m^2)	5×10^6
Acceleration due to gravity, g (m/s^2)	9.81

3 RESULTS AND DISCUSSION

3.1 *Permanent deformation*

Figure 2 illustrates the vertical permanent deformation in terms of ε_a with N at various σ'_3. It has been observed that ε_a increases with N at all σ'_3. However, ε_a decreases as σ'_3 increases. For instance, maximum ε_a of 18 % has been observed at σ'_3 = 10 kPa. Increasing σ'_3 to 30 kPa deduces ε_a to 11 %. A further increase of σ'_3 to 60 kPa resulted to ε_a of 8 %. Increasing σ'_3 from 60 kPa to 120 kPa did not show much influence on ε_a. Elevating σ'_3 to 240 kPa has further reduces ε_a to 6 % which is just 25 % less than that observed at σ'_3 = 60 kPa.

Figure 3 shows the response of ε_v with N at various σ'_3. At very low σ'_3 (e.g. 10 kPa), the ballast compresses during initial cycles (e.g. first 200 cycles) and then dilated causing high permanent vertical deformation as shown in Figure 1. However, as σ'_3 increases from 30 kPa to 240 kPa, the ballast compresses as N increases. Maximum compression observed at σ'_3 = 30 & 60 kPa are around 3 % and 4 % respectively. Increasing σ'_3 to 240 kPa results into a maximum volumetric compression of 4.5%.

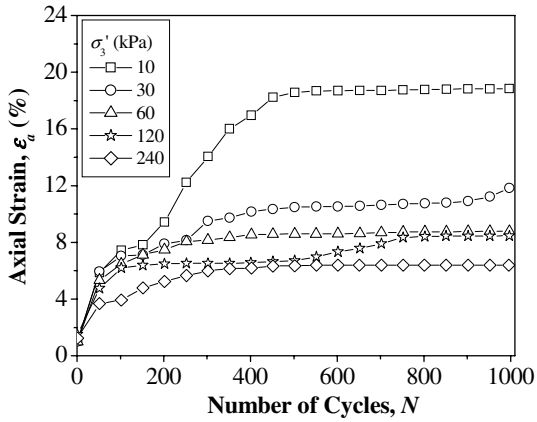

Figure 2. Variation of ε_a with N at different σ'_3

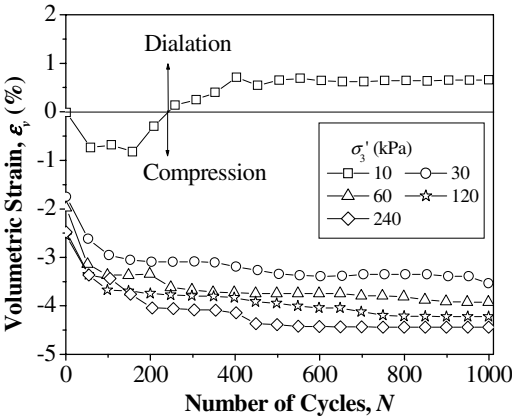

Figure 3. Variation of ε_v with N at different σ'_3

3.2 *Influence of bond breakage (B_r) on ε_a*

Figure 4 illustrates the influence of bond breakage (B_r) on ε_a with N. Breakage is expressed in terms of cumulative bond breakage (B_r), defined as the percentage of bonds broken in relation to the total number of bonds present in the assembly. Rapid increase in ε_a at initial cycles is mainly attributed to particle breakage (Figure 4). It can also be observed that during the first 200 cycles, B_r continuously increases with N. When the particle breaks, it acquires a greater chance to roll and slide which causes dramatic axial and volumetric deformation (Figures 2 & 3). When B_r stabilizes around N = 300, ε_a becomes almost constant. It can be seen clearly that from N = 300 to 500, ε_a is almost stable. At around 540 cycles, particles break more which increases ε_a. When the breakage of particles ceases around N = 700, ε_a again starts to stabilize. From these observations, it can be concluded that particle breakage is one of the major parameters controlling the permanent deformation of ballast.

3.3 *Micromechanical explanation of particle breakage*

Figure 5 illustrates the contact force (CForce chains) and particle displacement vectors, along with the locations of breakage. It can be seen from Figure 5 (a) that particle breakage is mainly concentrated along the principal CForce chains.

In Figure 5 (b), the particles are moving towards the direction of both the major and the minor principal stress directions during cyclic loading. Moreover, it is observed that bond breakage is concentrated mainly in the direction where the particles are moving. This phenomenon may be attributed to the decrease in coordination number of the particles associated with their movements which cause high tensile stresses in the particles. When the induced tensile stress exceeds the tensile strength of the parallel bonds, particle breakage occurs.

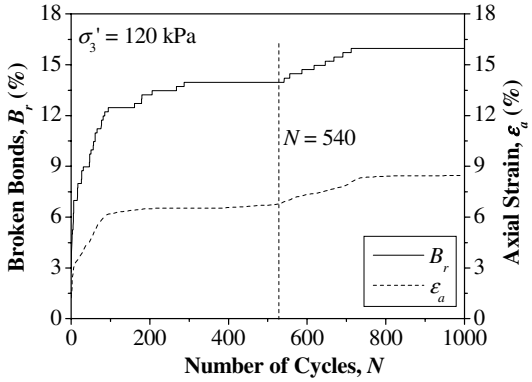

Figure 4. Effect of B_r on ε_a with N

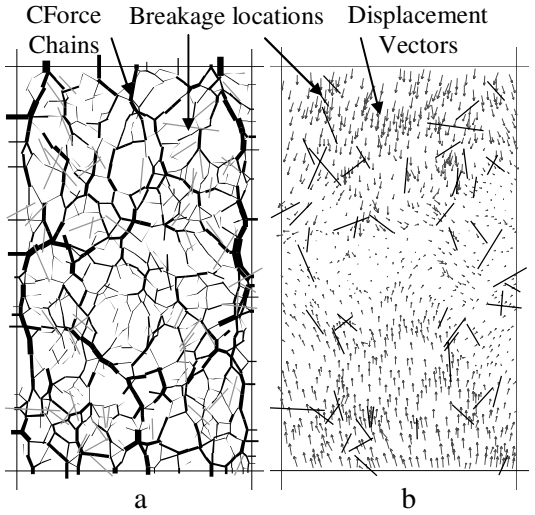

Figure 5. (a) CForce chains and location of particle breakage, (b) Displacement vectors and location of particle breakage at 60 kPa after 1000 cycles.

3.4 *Breakage behaviour*

Figure 6 explains the particle breakage behaviour at various values of σ'_3. For $\sigma'_3 < 30$ kPa, a very high B_r is observed. This is mainly caused by dilation of the assembly (Figure 3). Indraratna et al. (2005) have categorized this zone as 'Dilatant, Unstable Degradation Zone' (DUDZ), and reported that degradation is attributed mainly to the shearing and attrition of angular projections due to excessive axial and radial strains in this zone. With further increase in σ'_3, B_r is found to decrease, and it attains an optimum value in the range 30 kPa < σ'_3 < 75 kPa. This zone is named as the Optimum Degradation Zone (ODZ). Within this zone of confining pressure, an optimum particle configuration (packing arrangement) is attained thereby significantly reducing the dilative behaviour of the assembly and ε_a decreases significantly. This shows that rail tracks can benefit through reduced maintenance costs by slightly increasing the lateral confining pressure (i.e., less settlement and degradation of ballast). For $\sigma'_3 > 75$ kPa, B_r starts increasing (Figure 6), with a corresponding increase in ε_v and assigned a name CSDZ (Compressive, Stable, Degradation Zone) by Indraratna et al. (2005).

The ε_a in this zone is not much reduced when compared to ODZ as optimum packing arrangement of the particles is already attained. Figure 4 also compares the bond breakage (B_r) with ballast breakage index (*BBI*) developed by Indraratna et al. (2005). Although these two indices are distinctly different, they both measure the intensity of particle breakage. It is interesting to see that DEM results have

captured the same trends of breakage as those observed in the laboratory.

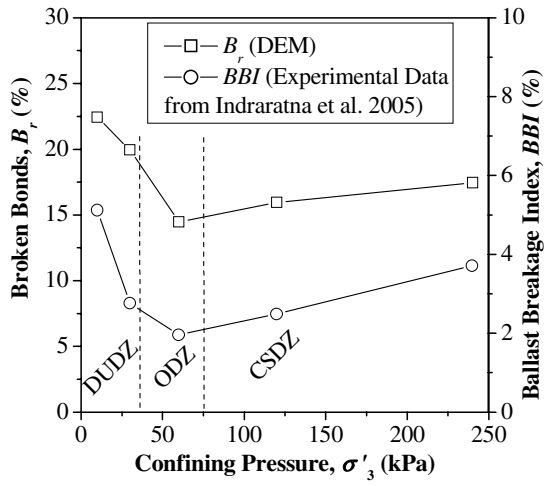

Figure 6. Particle breakage at various σ'_3 and comparison of breakage trends observed in the DEM with the experiment

4 CONCLUSIONS

A DEM simulation has been carried out to observe the effect of confining pressure on ballast behaviour under railway environments. Each ballast aggregate is modelled by clustering several smaller circular particles using parallel bonds. Breakages of these bonds are considered as particle breakage. The DEM results show that the axial strain and breakage are very high at very low confining pressure (< 30 kPa) owing to the dilative behaviour of the aggregates. With slight increase in confining pressure (≥ 30 kPa), substantial reduction in both the permanent deformation and degradation is observed. Beyond a confining pressure of 75 kPa, particle degradation increases without a significant decrease in permanent deformation. Moreover, the DEM results agree with previous laboratory findings of Indraratna et al. (2005) and verifies the role of confining pressure on the ballast behaviour. Particle breakage is found to be more pronounced in the direction of particle movement (i.e., in compliance with principal CForce chains). The recent results are currently being incorporated in the modified design of rail tracks in New South Wales, Australia through revised ballast and track standards.

ACKNOWLEDGEMENTS

The authors wish to thank Cooperative Research Centre for Railway Engineering and Technologies (Rail-CRC) for its financial support.

REFERENCES

Ben-Nun, O. & Einav, I. 2008. A refined DEM study of grain size reduction in uniaxial compression. The 12th International Conference of International Association for Computer Methods and Advances in Geomechanics (IACMAG), Goa, India, 702-708.

Bolton, M. D., Nakata, Y. & Cheng, P. 2008. Micro- and macro-mechanical behaviour of DEM crushable materials. Geotechnique, Vol. 58, No. 6, pp. 471 - 480.

Cheng, Y. P., Bolton, M. D. & Nakata, Y. 2004. Crushing and plastic deformation of soils simulated using DEM. Geotechnique, Vol. 54, No. 2, pp. 131-141.

Cundall, P. A. & Strack, O. D. L. 1979. A discrete numerical model for granular assemblies. Geotechnique, Vol. 29, No. 1, pp. 47-65.

Esveld, C. 2001. Modern Railway Track MRT Productions, The Netherlands.

Harireche, O. & McDowell, G. R. 2003. Descrete element modelling of cyclic loading of crushable aggregates. Granular Matter, Vol. 5, No., pp. 147-151.

Hossain, Z., Indraratna, B., Darve, F. & Thakur, P. K. 2007. DEM analysis of angular ballast breakage under cyclic loading. Geomechanics and Geoengineering, Vol. 2, No. 3, pp. 175 - 181.

Indraratna, B., Ionescu, D. & Christie, H. D. 1998. Shear behavior of railway ballast based on large-scale triaxial tests. Journal of Geotechnical and Geoenvironmental Engineering, Vol. 124, No. 5, pp. 439-449.

Indraratna, B., Lackenby, J. & Christie, D. 2005. Effect of confining pressure on the degradation of ballast under cyclic loading. Geotechnique, Vol. 55, No. 4, pp. 325-328.

Indraratna, B. & Salim, W. 2005. Mechanics of Ballasted Rail Tracks-A Geotechnical Perspective Taylor & Francis / Balkema, London, UK.

Itasca. 2003. Particle Flow Code in Two and Three Dimensions. Itasca Consulting Group, Inc., Minnesota, USA.

Lackenby, J., Indraratna, B., McDowell, G. & Christie, D. 2007. Effect of confining pressure on ballast degradation and deformation under cyclic triaxial loading. Geotechnique, Vol. 57, No. 6, pp. 527-536.

Lim, W. L. & McDowell, G. R. 2005. Discrete element modelling of railway ballast. Granular Matter, Vol. 7, No. 1, pp. 19.

Lobo-Guerrero, S. & Vallejo, L. E. 2006. Descrete element method analysis of railtrack ballast degradation during cyclic loading. Granular Matter, Vol. 8, No., pp. 195-204.

Lu, M. & McDowell, G. R. 2006. Discrete element modelling of ballast abrasion. Geotechnique, Vol. 56, No. 9, pp. 651-655.

Selig, E. T. & Waters, J. M. 1994. Track Geotechnology and Substructure Management Thomas Telford, London.

Standards Australia. 1996. Aggregates and rock for engineering purposes. Standards Association of Australia, 1-15.